Self-Assembled Nanogels of Cholesteryl-Modified Polysaccharides: Effect of the Polysaccharide Structure on Their Association Characteristics in the Dilute and Semidilute Regimes

Eri Akiyama,[†,‡,#] Nobuyuki Morimoto,[†,#] Piotr Kujawa,[§] Yayoi Ozawa,[†,||] Françoise M. Winnik,*[,§] and Kazunari Akiyoshi*[,†,||]

Institute of Biomaterials and Bioengineering, Tokyo Medical and Dental University, 2-3-10, Kanda-surugadai, Chiyoda-ku, Tokyo, 101-0062, Japan, Kao Corporation, Tokyo Research Lab., 2-1-3, Bunka, Sumida-ku, Tokyo, 131-8501, Japan, Department of Chemistry and Faculty of Pharmacy, University of Montreal, CP 6128 Succursale Centre Ville Montreal QC Canada H3C 3J7, and Center of Excellence Program for Frontier Research on Molecular Destruction and Reconstruction of Tooth and Bone, Tokyo Medical and Dental University, 2-3-10, Kanda-surugadai, Chiyoda-ku, Tokyo 101-0062, Japan

Received February 3, 2007; Revised Manuscript Received May 16, 2007

The assembly of cholesteryl derivatives of the highly branched polysaccharide mannan Mw = (5.2×10^4 g/mol) in dilute aqueous solution was investigated by ^{1}H nuclear magnetic resonance (NMR) spectroscopy, size-exclusion chromatography coupled with multiangle laser scattering (SEC-MALLS), dynamic light scattering (DLS), atomic force microscopy (AFM), fluorescence quenching, and fluorescence depolarization measurements. In the dilute regime, cholesteryl-bearing mannans (CHM) containing ~1 cholesteryl group per 100 mannopyranose units formed nanogels with a hydrodynamic radius (R_H) of ~20 nm containing ~8 macromolecules held together via hydrophobic nanodomains consisting of ~9 cholesteryl groups. Their density Φ_h (~0.02) was significantly lower than the density (~0.16) of nanogels formed by a cholesteryl derivative of the linear polysaccharide pullulan (CHP) of identical molar mass and level of cholesteryl substitution. In the semidilute regime, CHM nanogels formed a macrogel network for concentrations higher than 12.5% w/w, whereas CHP nanogels underwent macrogelation only above a threshold concentration of 8.0% w/w, as revealed by oscillatory and steady-shear viscosity measurements. The differences in the solution properties of CHM and CHP reflect differences in their assembly on the molecular level, in particular, the size and number of hydrophobic nanodomains and the hydration level. They are attributed to differences in the mobility of the cholesteryl groups which, itself, can be traced to the fact that in CHM the cholesteryl groups are predominantly linked to short oligomannopyranose branches, whereas in CHP they are linked to the polymer main chain. Our study provides a novel means to nanoengineer polysaccharide nanogels which may find unique biotechnological applications.

Introduction

The self-assembly of polysaccharides in water provides ready access to waterborne supramolecular architectures[1,2] which have found numerous applications as chromatographic systems,[3] sensing devices,[4] drug delivery systems,[5] or gene therapy vectors. While oppositely charged polysaccharides associate readily as a result of electrostatic attraction,[2] interactions among neutral polysaccharides tend to be weaker, or nonexistent, and it is necessary to modify their skeleton with fragments able to trigger assembly. A convenient strategy consists of linking hydrophobic substituents to a highly water-soluble, nontoxic, polysaccharide to induce the formation of nanoparticles held together via hydrophobic nanodomains. The impact of the hydrophobic group structure and of the degree of substitution on the physicochemical properties of the resulting nanoparticles has been investigated in detail for several polysaccharides, leading to design rules with respect to the hydrophobes. The effect of the carbohydrate framework itself on the assembly of amphiphilic polysaccharides is less well understood and is often ignored.

We reported several years ago that pullulan, a linear homopolymer of glucopyranose linked by α(1 → 4) and α(1 → 6) linkages in a ratio of 2:1, bearing a small number of cholesteryl residues (cholesteryl pullulan or CHP, Figure 1) forms stable nanoparticles in water.[6,7] The CHP nanoparticles range in size from 20 to 30 nm with excellent size monodispersity. They behave like hydrated nanogels held together via cholesteryl nanodomains acting as physical cross-linking points. The size, density, and number of cross-linking domains within the nanoparticles are regulated by the number and structure of the hydrophobic groups.[8] CHP nanogels undergo hierarchical self-assembly, forming macroscopic gels in semidilute solutions.[9] They also form complexes with various water-soluble polymers, such as cholesterol-bearing polyamino acids,[10] alkyl group modified poly(*N*-isopropylacrylamide),[11] deoxycholic acid-modified glycol chitosan,[12] deoxycholic acid-modified

* To whom correspondence should be addressed. F.M.W.: phone: 514-340-5179; fax: 514-340-3245; e-mail: francoise.winnik@umontreal.ca. K.A.: phone: 81-3-5280-8020; fax: 81-3-5280-8027; e-mail: akiyoshi.org@tmd.ac.jp.

† Institute of Biomaterials and Bioengineering, Tokyo Medical and Dental University.

‡ Kao Corporation.

§ University of Montreal.

|| Center of Excellence Program for Frontier Research on Molecular Destruction and Reconstruction of Tooth and Bone, Tokyo Medical and Dental University.

# These authors contributed equally to this work.

10.1021/bm070136q CCC: $37.00
Published on Web 07/14/2007

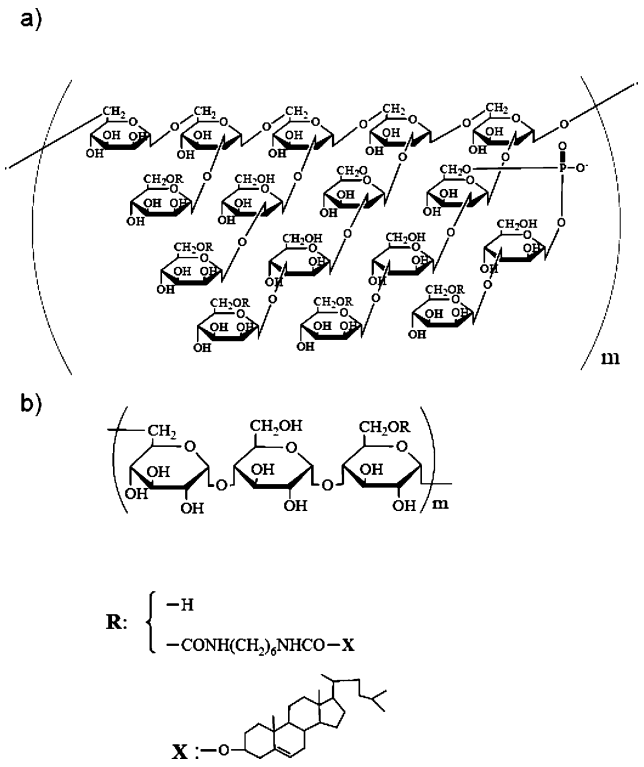

Figure 1. Chemical structures of (a) CHM and (b) CHP.

heparin,[13] and bile acid bearing dextran.[14] Proteins are readily entrapped within nanogels and can be released in their native form to the environment,[15] a property taken to advantage in the design of specific artificial molecular chaperone.[16,17] The unique characteristics of the nanogels offer applications in many biotechnological areas, in particular, as drug delivery systems.[17−19]

The breadth of applications of CHP nanogels prompted us to undertake a systematic investigation of the impact of the polysaccharide structure on the physicochemical properties of their cholesteryl-modified analogues. We report here the solution properties of cholesteryl derivatives of mannan, a polymer of mannose (CHM, Figure 1). Specifically, we used yeast mannan, extracted from *Saccharomyces cerevisiae*, which is a highly branched polysaccharide with α-(1 → 2)- and α-(1 → 3)-linked mono-, di-, and trimannopyranose side chains with phosphodiester-linked side chains (2.6 phosphorus in 100 mannopyranose units) attached to the backbone of α-(1 → 6)-linked mannopyranoses.[20−22] Cholesteryl groups were linked to the mannan framework via a small alkyl linker, similarly to the case of cholesteryl-modified pullulan. The level of hydrophobe incorporation was chosen to be of the same order of magnitude as in the case of a CHP sample for which a full characterization has been reported previously. We present here a study of the solution properties of the new cholesteryl−mannan in water in the dilute and semidilute regimes, using static and dynamic light scattering, ^{1}H NMR spectroscopy, fluorescence spectroscopy, and rheology. We provide also an overview of the solution properties of cholesteryl−pullulan nanogels in water using published data and some additional experimental results as needed. Taken together, the experimental results unveil marked differences between mannan- and pullulan-based nanogels which we attribute to the structural and chemical differences between the two polysaccharides and suggest design guidelines toward application-specific polysaccharide-based nanogels.

Experimental Section

Materials. The mannan (Mw = 5.21 × 10^4, M_w/M_n = 1.27) from *Saccharomyces cerevisiae* was purchased from Sigma-Aldrich (St. Louis, MO). The phosphodiester linkage contains about 2.6 phosphorus in 100 mannopyranose units determined by phosphorus analysis. Pullulan (M_w = 5.04 × 10^4 g/mol, M_w/M_n = 1.30) was purchased from Hayashibara Biochemical Laboratory, Inc. (Okayama, Japan). The cholesteryl group bearing mannan (CHM) and pullulan (CHP) were synthesized as described previously.[6] The degree of substitution of cholesteryl groups in CHM and CHP were, respectively, 1.0 and 1.1 per 100 sugar units. Pyrene was purchased from Accu Standard Inc. (New Haven, CT). Diphenylhexatriene (DPH) was purchased from Aldrich Chemicals (Milwaukee, WI). Cetylpyridinium chloride (CPC) was purchased from Tokyo Chemical Industry Co., Ltd. (Tokyo, Japan). Water was deionized by a Milli-Q (Millipore, Bedford, MA) water purification system. All other reagents were commercially available and were used without further treatment.

Size-Exclusion Chromatography (SEC)−Multiangle Laser Scattering (MALLS) Measurements. Molecular weights and molecular weight distributions were determined by SEC conducted with a Tosoh Ltd. (Tokyo, Japan) chromatography system composed of a DP-8020 dual pump, a CO-8020 column oven, an RI-8020 refractive index detector, and a DAWN E MALLS detector (Wyatt Technology, Santa Barbara, CA), 30 mW, λ = 690 nm, using a G-4000SW$_{XL}$ column (Tosoh Ltd.) eluted at 20 °C with aqueous NaCl (50 mM). Absolute molecular weights were determined using a d*n*/d*c* value of 0.136 mL/g, determined with an OPTILAB DSP differential refractometer (wavelength: 690 nm), for mannan and CHM. Solutions for analysis were passed through a 0.45 μm filter before injection.

Dynamic Light Scattering (DLS) Measurements. DLS measurements were carried out at 25.0 ± 0.1 °C with a Zetasizer nano ZS instrument (Malvern Instruments, Malvern, United Kingdom) at a wavelength of 632.8 nm and a 173° detection angle. The hydrodynamic radius of the CHM nanogels was determined with a Laplace inversion program (CONTIN). The nanogel solutions (5 mg/mL) were centrifuged (14 000 rpm, 40 min) and were passed through a PVDF filter (pore size, 0.45 μm) prior to measurements.

Atomic Force Microscopy (AFM) Measurements. A gold substrate cleaned by ultrasonication in acetone and in distilled water was placed in an aqueous CHM solution (1.0 mg/mL) for 1.5 h. The surface was rinsed in water, and excess solvent was removed under a gentle stream of N_2. The surface was observed with an atomic force microscope (AFM) (SPI300, Seiko Instruments Inc., Chiba, Japan) equipped with a Si Probe (SI-DF20, Seiko Instruments Inc.) with a spring constant of 15 N/m. The nanogel size distribution was determined by measuring the size of 100 nanogels and by using an NIH Image software package.

Fluorescence Quenching Experiments. Fluorescence spectra were recorded with an FP-750 spectrofluorimeter (JASCO Corporation, Tokyo, Japan). The slit widths were set at 5 nm for excitation and 1 nm for emission. The excitation wavelength was 339 nm and measured 384 nm. Solutions for analysis were prepared as follows. A small amount of a solution of pyrene in acetone (1 × 10^{-4} M) was placed in several vials. The acetone was evaporated with a stream of argon to form a thin film on the bottom of the vials. CHM nanogel solutions of various concentrations (3.0−8.0 mg/mL) were placed in the vials such that the concentration of pyrene was 1.0 × 10^{-6} M in each sample, and the cholesteryl concentration ranged from 2.0 × 10^{-7} to 5.2 × 10^{-7} M. The solutions were stirred at room temperature overnight. Aliquots of an aqueous solution of CPC (1.3 × 10^{-6} M) were added to the CHM/Py solutions immediately prior to fluorescence measurements. The number of cholesteryl moieties associated in a nanodomain (N_{ch}) was estimated using the steady-state fluorescence-quenching technique,[23] for which the ratio (I/I_o) of the fluorescence intensities in the presence and in the absence of a quencher (Q) is related to [Q], the quencher concentration, and to [M], the concentration of cholesteryl domains, by eq 1:

$$\ln \frac{I_o}{I} = \frac{[Q]}{[M]} \text{ with } N_{ch} = \frac{[\text{cholesteryl}]}{[M]} \quad (1)$$

A plot of $\ln(I_0/I)$ against [Q] gives a straight line, the slope of which corresponds to $[M]^{-1}$.

Fluorescence Anisotropy Measurements. Fluorescence anisotropy (r) measurements were performed on a Varian Cary Eclipse spectrometer equipped with two Glan−Thompson polarizers in the L-format configuration. The temperature of the sample fluid was controlled using a water-jacketed cell holder connected to a Cary circulating water bath and was measured with a thermocouple immersed in a water-filled cell placed in one of the four cell holders in the sample compartment. The temperature of the sample was 25 °C. The slit settings were 5 nm for both excitation and emission. The excitation and emission wavelengths were set at 340 and 426 nm, respectively.

The fluorescence anisotropy was calculated from the relationship

$$r = \frac{I_{vv} - GI_{VH}}{I_{vv} - 2GI_{VH}} \quad (2)$$

where $G = I_{VH}/I_{HH}$ is an instrumental correction factor and I_{VV}, I_{VH}, and I_{HH} refer to the emission intensities at 426 nm polarized in the vertical or horizontal planes (second subindex). The values reported in the text are averages of three measurements (standard error ± 0.01). Samples for analysis were prepared as follows. An aliquot of a stock solution of 1,6-diphenyl-1,3,5-hexatriene (DPH, 1 mM) in tetrahydrofuran was placed in a flask. The solvent was removed under a stream of nitrogen. Water was added in the flask such that the final DPH concentration was 1 μM. Stock solutions of CHP and CHM (5.0 mg/mL) were prepared by dissolving each polymer in aqueous DPH (1 μM). The mixture was stirred vigorously at room temperature overnight. It was subjected to ultrasonication (40 W, 15 min) using a probe type sonicator. Solutions for analysis were prepared from the aqueous stock solutions of CHP and CHM samples containing DPH. Solutions were filtered through 0.45 and 0.22 $^1/_4$m PVDF filters prior to measurements.

Fluorescence Lifetime Measurements. Fluorescence lifetimes were measured on a Fluoro-Tau-3 multifrequency phase-modulation fluorimeter (Jobin-Yvon Horiba Inc.). The excitation light from 450 W xenon lamp was modulated with a Pockels cell. Phase and modulation values were determined relative to a glycogen aqueous solution. The excitation wavelength was set at 426 nm. The frequency of the analyzing light was chosen in the range of 5−200 MHz. The temperature of the sample was constant and equal to 25 °C.

Fluorescence data were analyzed with the Datamax Spectroscopy software on the basis of GRAM/32 from Galactic Ind. In all cases, data could be fitted to a single- or double-exponential decay law, $\sum_{i=1}^{n} a_i \exp(-t/\tau_i)$ where a_i and τ_i are the pre-exponential factor and the lifetime of the ith component ($i = 1$ or 2), respectively. The fractional contribution (f_i) of each decay time to the steady-state intensity was calculated as $f_i = (a_i\tau_i)/(\sum_j a_j\tau_j)$. In the case of double-exponential decay, the average lifetime ($\bar{\tau}$) equals $\bar{\tau} = f_1\tau_1 + f_2\tau_2$. The goodness of the fit was determined by the χ^2 value, which was $\chi^2 = 1.5-2.6$, and an examination of the residuals. Solutions for analysis were prepared in the same way as for anisotropy experiments described above.

NMR Measurements. Proton NMR spectra of aqueous solutions of the nanogels (5 mg/mL) were recorded with a 500 MHz Bruker Avance spectrometer (Bruker BioSpin GmbH, Rheinstetten) using a deuterium lock. Spectra were recorded at 25, 40, and 70 °C.

Rheological Measurements. Oscillatory measurements and steady-shear viscosity measurements were performed with a Modular Compact Rheometer MCR300 (PHYSICA Messtechnik GmbH) in the cone-plate geometry (CP50-2: angle 2°, diameter 50 mm or CP75-1: angle 1°, diameter 75 mm) at 25 °C. All data were collected in the linear viscoelastic region. The sample was covered by a reservoir filled with water during the measurements to prevent the evaporation of water.

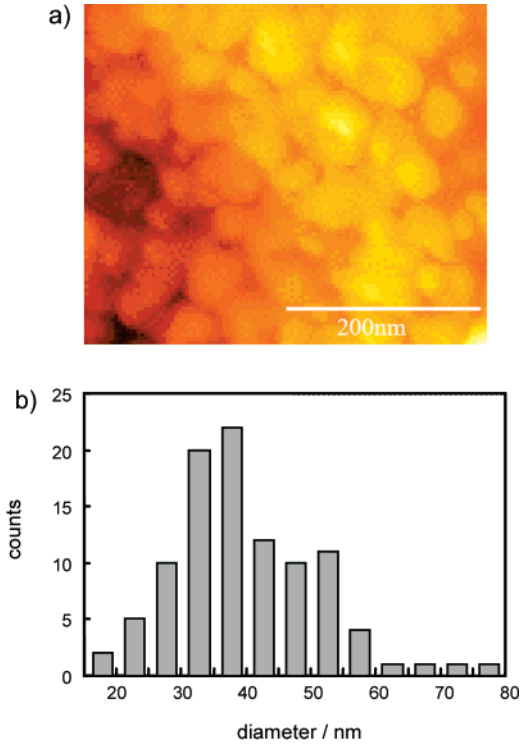

Figure 2. (a) AFM image of CHM nanogels and (b) the size distribution.

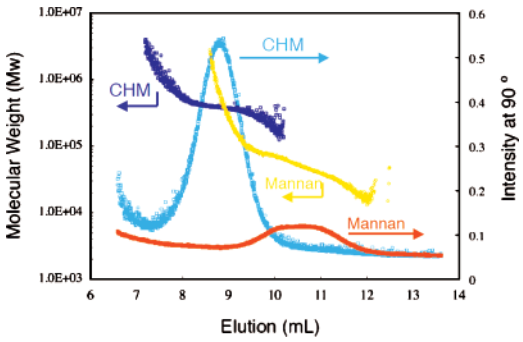

Figure 3. Molecular weight distribution of CHM nanogels and of mannan determined by SEC-MALLS.

Results and Discussion

Properties of Cholesteryl−Mannan in Dilute Solution. The presence of self-assembled structures in aqueous solutions of CHM was detected readily by a dynamic light scattering analysis which revealed the presence of nanoparticles with a hydrodynamic radius (R_H) of 19.3 ± 0.5 nm. It was confirmed by atomic force microscopy (AFM) imaging of a specimen obtained by deposition on a gold surface of an aqueous CHM solution (1.0 mg/mL) and subsequent drying at 20 °C under a gentle flow of N_2. The micrograph (Figure 2a) presents an ensemble of densely packed spherical and oblong particles. The number-average diameter of the particles is 40 ± 11 nm (Figure 2b), a value of the same order of magnitude as the size of the nanogels in solution determined by DLS. The characteristics of CHM nanoparticles in dilute aqueous solution were investigated also by size exclusion chromatography coupled with multiangle laser scattering. The elution profile of CHM particles in water was unimodal and of low polydispersity in size ($M_w/M_n = 1.09$) (Figure 3). The apparent molecular weight of the species detected is 4.11×10^5 g/mol, a value much larger than the molecular weight of one mannan chain before modification which is 5.21×10^4 g/mol as determined via SEC-MALLS

measurements. Thus, the CHM nanoassemblies formed in water resist disintegration upon elution though the SEC columns. Taking the ratio of the apparent molecular weight of CHM in water to the molecular weight of a single CHM chain, one can estimate that the nanoparticles have an aggregation number (N_{CHM}) of ~7.5. From the experimental R_H and M_w values, one can calculate the average polymer density (Φ_H) within a CHM nanoparticle defined by eq 3 where N_A is Avogadro's number:

$$\Phi_H = \left(\frac{M_w}{N_A}\right)\left(\frac{4}{3}\pi R_H^3\right)^{-1} \quad (3)$$

The average polymer density is ~0.02 g/mL, implying that the CHM nanoparticles consist of only 2 wt % of polysaccharide with 98 wt % of water and that, consequently, they will exhibit hydrogel-like properties.

On the basis of our experience with CHP nanogels, we anticipated that each CHM nanoparticle will contain hydrophobic nanodomains surrounded by a highly hydrated polysaccharide phase. We employed fluorescence spectroscopy to ascertain the presence of hydrophobic nanodomains and to assess their size and their local microviscosity. Three types of fluorescence probe measurements were carried out. First, we used pyrene (Py) to detect the presence of hydrophobic domains and assess their micropolarity. The method is based on the sensitivity of the fine structure of the Py emission to the polarity of the probe microenvironment. As "polarity scale", one usually measures the ratio I_1/I_3 of the intensity of the emission at 377 nm (I_1) to that of the emission at 387 nm (I_3).[24] The ratio takes a value of ~1.70 when Py is exposed to a polar medium such as water. It is much lower (1.0−1.1) in the case of Py dissolved in alkanes or within the hydrophobic core of surfactant micelles. The emission of Py in solution of CHM nanogels was ~1.01, a value typical of Py in a hydrophobic medium.

Next, we applied a fluorescence-quenching technique to estimate the number of cholesteryl moieties in each hydrophobic nanodomain. In this approach, solutions of the nanogels containing Py solubilized within the cholesteryl domains are treated with increasing concentrations of a hydrophobic quencher of fluorescence. Analysis of the data according to the Stern−Volmer formalism (see Experimental Section) yields the aggregation number of the hydrophobic domains.[25] The technique has been successfully applied to determine the aggregation number of surfactant micelles,[26] of microdomains in solutions of polysoaps,[27] and of the cholesteryl nanodomains of CHP.[3] Plots of the changes of $\ln(I_0/I)$ of where I_0 is of the Py emission intensity in the absence of quencher and the emission of Py in the presence of cetylpyridinium chloride (CPC), as a function of CPC concentration are presented in Figure 4 for CHM solutions of various concentrations. Straight lines were obtained in all cases. From their slope and using eq 1 (Experimental Section), the mean aggregation number of the cholesteryl moiety in CHM nanogels, N_{ch}, was estimated to be 8.8 ± 0.4. Recalling that each nanogel consists on average of 7.5 macromolecules, and knowing the number of cholesteryl groups per chain, one can determine that each CHM nanogel contains about 25 cholesteryl moieties. Thus, on average, each nanogel particle can be depicted as containing ~2.9 independent cholesteryl nanodomains (n_{domain}), each formed by clustering of ~8.8 cholesteryl groups.

To estimate the microviscosity of the hydrophobic nanodomains, we carried out fluorescence depolarization measurements with CHM solutions doped with diphenylhexatriene (DPH), a hydrophobic probe preferentially localized within

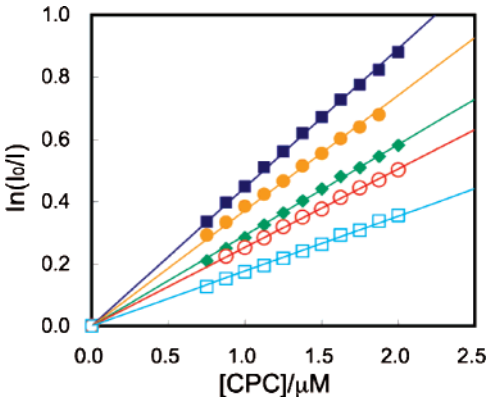

Figure 4. $\ln(I_0/I)$ of pyrene fluorescence as a function of the CPC concentration in the presence of CHM. Beginning at the top: 3, 4, 5, 6, and 8 mg/mL of CHM, [Py] = 1×10^{-6} M. Lines are best fits of eq 1 to the data.

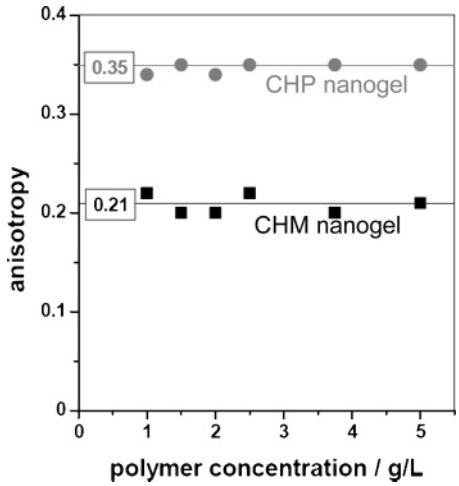

Figure 5. Fluorescence anisotropy of DPH as a function of polymer concentration for CHM and CHP nanogel solutions.

Table 1. Fluorescence Lifetimes of DPH in Aqueous Solutions of CHP and CHM

sample	concentration/g/L	τ_1/ns	f_1	τ_2/ns	f_2	$\bar{\tau}$/ns
CHM	1.0	7.4	0.85	1.0	0.15	6.4
	2.5	5.4	0.86	0.6	0.14	4.7
	5.0	4.4	0.90	0.4	0.10	4.0
CHP	1.0	4.9	0.92	0.9	0.08	4.6
	2.5	3.6	0.92	0.6	0.08	3.3
	5.0	2.9	0.91	0.3	0.09	2.7

hydrophobic environments.[27] The measurements were carried out with CHM solutions in the 1−5 mg/mL concentration range, yielding an anisotropy (r) of ~0.21, independently of polymer concentration (Figure 5). This anisotropy value sensed by DPH molecules in CHM is of the same magnitude as values determined for DPH in lipid bilayers (0.20−0.30),[28,29] hydrophobically modified water-soluble polymers (0.20−0.28),[30] and micelles of diblock polymers (0.20−0.27).[31] The mobility of hydrophobic segments in the case of the CHM nanogels is thus in the range usually observed for amphiphilic polymers and related systems.

Control frequency−domain fluorescence measurements were carried out as a function of nanogel concentration and structure. In all cases, the DPH decay followed a double-exponential law, with a long-lived main component (τ_1 = 7.5−3 ns) and a minor short-lived component (τ_2 < 1 ns) (Table 1). The presence of two lifetimes for DPH in CHM solutions may be an indication

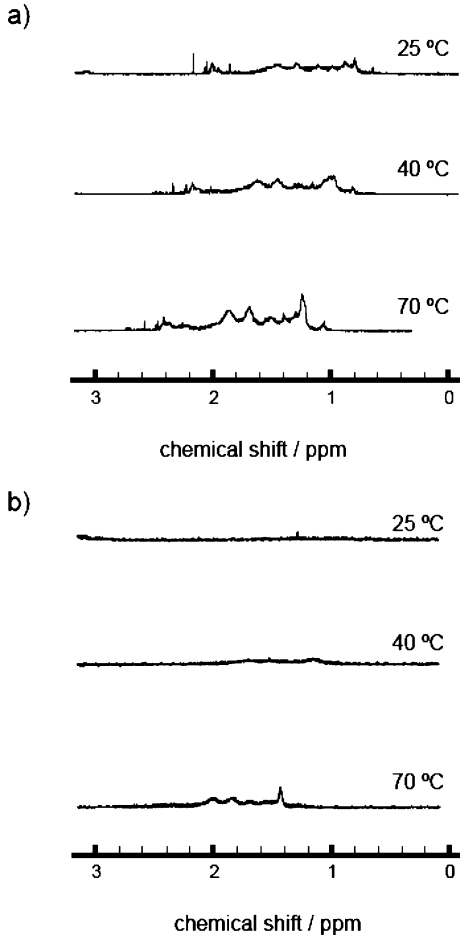

Figure 6. ^{1}H NMR spectra of (a) CHM nanogels and (b) CHP nanogels in D_2O at 25, 40, and 70 °C.

Table 2. Solution Properties of Nanogels

sample	M_w	$N_{polysaccharides}$	R_H (nm)	M_w/M_n	Φ_H (g/mL)	N_{ch}
CHM nanogel	4.1×10^5	7.5	19.5	1.09	0.02	8.8 ± 0.4
CHP nanogel	6.2×10^5	11	11.6	1.03	0.16	4.4 ± 0.5

of a distribution of DPH molecules in water or in the hydrophilic sections of the nanogels and in the hydrophobic nanodomains.

^{1}H NMR spectra of CHM nanogels were measured in D_2O at 25, 40, and 70 °C (Figure 6a). The spectrum recorded at 25 °C presents signals from δ 0.6 to δ 2.0 ppm, characteristic of the cholesteryl moiety and of the hexamethylene spacer between the cholesteryl group and the mannan glucopyranosyl units. The signals due to the resonance of the cholesteryl protons become sharper as the solution temperature increases, indicating a temperature-induced enhancement of the mobility of the cholesteryl moieties in the hydrophobic domains.

Properties of CHM and CHP Nanogels. From the series of measurements described thus far, we can conclude that the self-assembly of CHM in water under dilute conditions follows the same patterns as cholesteryl pullulans (CHP) and that the general features of the two types of nanogels are quite similar. However, closer examination of the two systems reveals striking differences. To facilitate the comparison, we present in Table 2 the main structural characteristics of CHM nanogels in water under dilute conditions, together with the corresponding values previously reported for aqueous solutions of a CHP sample of nearly identical molecular weight ($M_w = 5.0 \times 10^4$) and degree of cholesteryl groups substitution. We note that (1) the density of CHM nanogels is smaller than that of CHP nanogels; (2) the aggregation number of CHM (7.5) is smaller than that of CHP (11.0); (3) the hydrodynamic radius of CHM nanogels is ~1.7 times larger than that of CHP nanogels; and (4) the aggregation number of cholesteryl moieties (N_{ch}) in CHM nanogels (~8.8) is about twice than that of CHP nanogels (~4.4).

From fluorescence depolarization measurements carried out with DPH loaded CHP solutions under conditions similar to those used in the case of CHM, we determined the anisotropy value of DPH in CHP to be ~0.35, independently of the CHP concentration (Figure 5). This value is close to the limiting anisotropy ($r_0 = 0.39$) of DHP.[28] The Perrin equation (eq 4), where T_τ is the temperature, k_B is the Boltzman constant, and V_o is the probe volume, allows one to use the anisotropy values r to estimate the effective viscosity η_{eff} sensed by the probe

$$\frac{r_0}{r} = 1 + \frac{k_B T_\tau}{\eta_{eff} V_0} \tag{4}$$

The $\eta_{eff,CHP}$ value calculated using eq 4 is higher than $\eta_{eff,CHM}$ by a factor of ~5.8. Thus, the cholesteryl clusters are significantly more rigid in CHP nanogels compared to CHM nanogels. This conclusion is corroborated by results from ^{1}H NMR spectroscopy. Recall (Figure 6a) that the ^{1}H NMR spectrum of CHM nanogels in D_2O at 25 °C presents distinct, albeit slightly broad, signals attributable to the resonances of the cholesteryl protons, an indication that the cholesteryl moieties preserve significant mobility within the hydrophobic nanodomains. In contrast, the ^{1}H NMR spectrum of CHP nanogels in D_2O at 25 °C (Figure 6b) exhibits no signals corresponding to the cholesteryl protons, implying that the motion of the cholesteryl moieties within CHP nanogels is highly restricted.

The higher mobility of the cholesteryl groups in CHM nanogels, compared to CHP nanogels, is intriguing. One of the plausible explanations is that it is a consequence of differences in the chemical structure of the two modified polysaccharides although they were prepared under identical experimental conditions by reaction of cholesteryl isocyanate with hydroxyl groups of the polysaccharide. Primary hydroxyl groups are known to react faster than secondary hydroxyl groups in our synthetic protocol. Pullulan has primary OH groups on the C6 position of each unit. These are expected to react faster and, consequently, most of the cholesteryl groups will be linked directly to the main chain of this linear polysaccharide. Mannan, in constrast, has no free primary OH groups directly linked to the main chain, since these groups participate in the formation of the α-(1 → 6) linkage between mannopyranose groups. Free primary OH groups exist only on the C6 positions of the short oligosaccharide branches distributed along the mannan main chain. Therefore, most cholesteryl groups are probably attached to the mannan main chain via a small oligomannose linker. Such oligosaccharide spacers give the cholesteryl groups enhanced mobility. Moreover, the cholesteryl groups linked to such short branches are expected to experience less steric hindrance than groups linked directly to the main chain, a circumstance that will facilitate their association and may be responsible for the larger number of cholesteryl groups per nanodomains in CHM nanogels compared to CHP nanogels. A pictorial representation of the self-assembly of CHM and CHP nanogels is given in Figure 7. To assess if the enhanced mobility of the CHM cholesteryl groups also affects internanogel association in the semidilute regime, we carried out a comparative study of the rheological properties of CHM and CHP nanogels described next.

Properties of Cholesteryl−Mannans and Cholesteryl−Pullulans in Semidilute Solution. First, we measured the

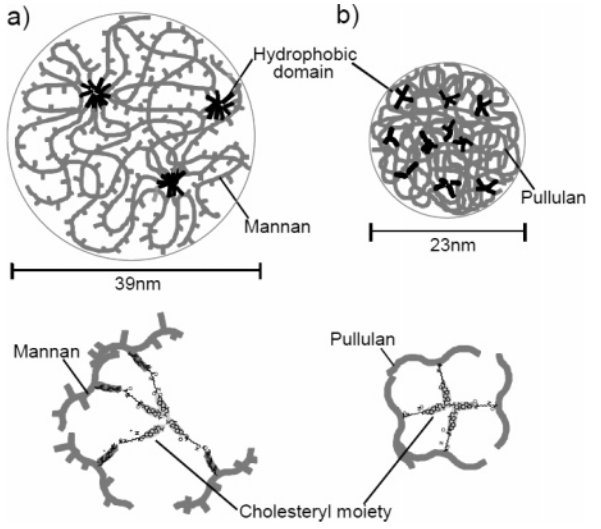

Figure 7. Schematic illustrations of (a) CHM nanogel and (b) CHP nanogel.

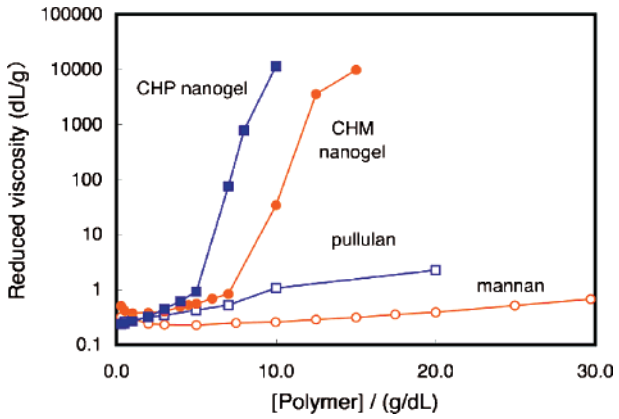

Figure 8. Viscosity as a function of concentration of CHP, CHM, pullulan, and mannan solutions.

steady-shear viscosity of CHM, CHP, mannan, and pullulan solutions in water of various concentrations (C). The reduced viscosity of the samples was calculated using the relation $\eta_{red} = (\eta_{rel} - 1)/C$, where η_{rel} is the relative plateau viscosity. The corresponding Huggins plots are shown in Figure 8. For solutions of concentration larger than 3 g/dL, the viscosity of mannan and CHM nanogel solutions was lower than that of pullulan and CHP nanogel solutions, respectively.

The viscosity of the CHM and CHP nanogel solutions increases with increasing concentration, signaling the formation of macroscopic gelation. Surprisingly, the viscosity enhancement is steeper in the case of CHP nanogels compared to CHM nanogels such that, for example, the viscosity of a 10% w/w CHP solution is ~100 times that of a 10% w/w CHM solution (see Figure 8). From a mechanistic view point, the viscosity enhancement is due to the association of nanogels by interparticle hydrophobic interactions between the cholesteryl units. Recall that individual CHP nanogels comprise on average 3 times more hydrophobic nanodomains than CHM nanogels. Thus, the probability of nanogel association is larger in semidilute solution of CHP compared to CHM. Moreover, the formation of interparticle links is accompanied by a relief of the chain constraints within particles and is entropically favored. This driving force toward gelation is weaker for CHM nanogels which have a looser inner structure than CHP particles, and there is also electrostatic repulsion between CHM nanogels. In the very low concentration regime (below 3 g/dL), the reduced viscosity of mannan and CHM nanogel solutions increases

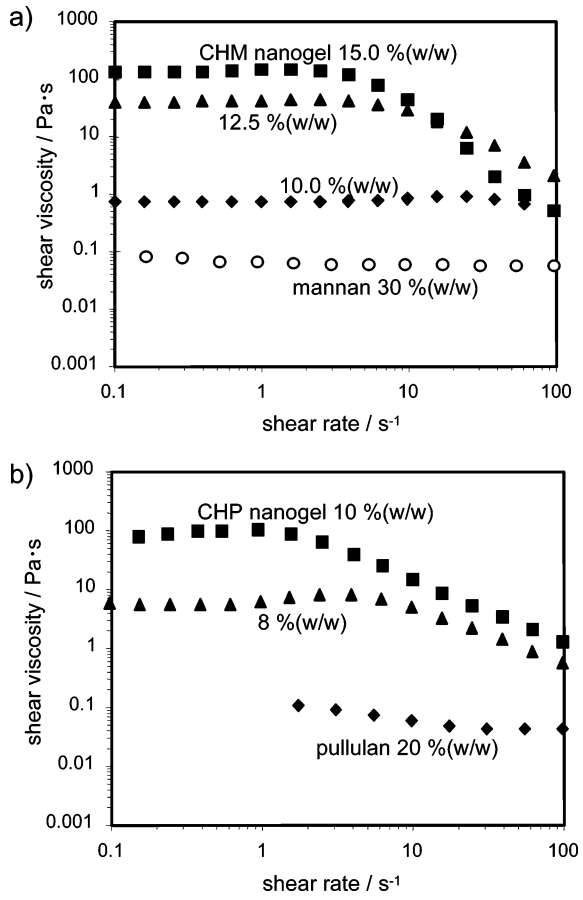

Figure 9. Shear rate dependence on steady-shear viscosity of (a) CHM nanogels and mannan and (b) CHP nanogels and pullulan.

unlike the case of pullulan and CHP samples for which the intrinsic viscosity decreases slightly with decreasing concentration. The behavior of mannan and CHM solutions is typical of polyelectrolyte solutions in water and reflects the presence of a small number of negatively charged phosphodiester units.

Next, we compared the steady-shear viscosity as a function of shear rate for solutions of mannan, pullulan, CHM, and CHP of increasing concentration (Figure 9). A pronounced shear-thinning behavior was observed in the case of CHM and CHP solutions of concentration equal to 12.5% w/w and 8% w/w, respectively. Solutions of mannan and of pullulan show no shear-thinning characteristics up to a concentration of 30% w/w. For CHP or CHM nanogel solutions, in analogy with other associative polymers, the non-newtonian behavior results from hydrophobic interactions between gel particles.

Frequency sweeps of the storage (G') and loss (G'') moduli of the same CHM, CHP, mannan, and pullulan solutions are presented in Figure 10. In the case of CHM nanogels (Figure 10a), the loss modulus G'' reaches a maximum value for 12.5 and 15.0% w/w CHM samples. The dissociation of the cholesteryl groups and subsequent breakup of the particles are believed to be the main contributors to this relaxation process. The value of G' recorded for 12.5 and 15.0% w/w CHM samples reached a plateau in the high-frequency regime (at $\omega \sim 100$ rad·s^{-1}), where the CHM gel behaves like an elastic body. For CHM samples of increasing concentration, the plateau value reached by G' increases, while the frequency corresponding to the crossover between G' and G'' shifts to lower values (15% w/w: 3 rad·s^{-1}, 12.5% w/w: 5 rad·s^{-1}, 10% w/w: 100 rad·s^{-1}). This suggests that the elasticity component becomes the predominant relaxation process as the system becomes more concentrated and, consequently, the network structure becomes more and

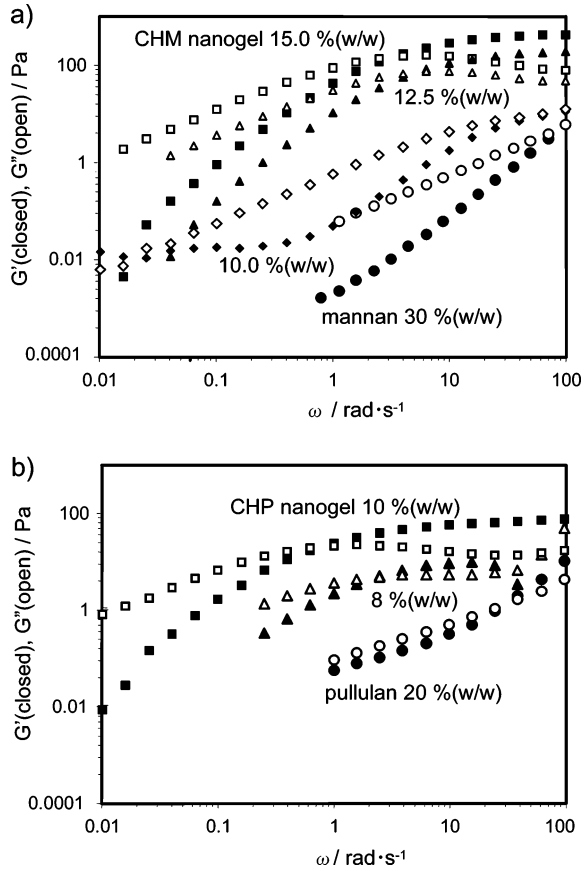

Figure 10. Frequency sweep of storage (G') and loss (G'') moduli of (a) CHM nanogels and mannan and (b) CHP nanogels and pullulan solutions at 25 °C.

more extensive. As CHM concentration increases, an increasingly large number of individual nanogels enter in contact via multiple cholesteryl clusters triggering further polymer chain interpenetration. These processes enhance polymer cross-linking, resulting in the formation of a gel network.

For systems of CHP nanogels (10% w/w), the G'/G'' crossover occurs in the $\omega < 1$ rads^{-1} frequency regime (Figure 10b), that is, lower than in the case of CHM gels ($\omega = 5$ rads^{-1}, 12.5% w/w). The plateau value of G' for CHP is higher than that of CHM. This observation implies that the cross-linking points of CHP gels are more stable and that the number of cross-linking points in CHP gels is larger than in the case of the CHM gel, reflecting differences in either the mobility of the cholesteryl groups or the stability of the hydrophobic nanodomains as a consequence of differences in the structure of the two polysaccharides as previously discussed. Thus, the mobility of the cholesteryl groups in the nanogels greatly affects the macroscopic association of the nanogels and the dynamics of the macrogel formed in the semidilute regime.

Conclusion

Hydrophobically modified polysaccharides obtained by attachment of cholesteryl groups to the highly branched mannan form highly hydrated nanogels (CHM) in water through the association of cholesteryl moieties following a pattern exhibited by other modified polysaccharide such as cholesteryl pullulan (CHP). A comparative study of the two types of nanogels has revealed that the structure and level of hydration of the polysaccharide chain significantly affect the microscopic structure of the self-aggregates and the microviscosity of the hydrophobic domain within the nanogels. Through earlier work, we have demonstrated that tailor-made functional nanogels can act as building blocks to create novel biomaterials through the controlled self-association of functional associating polymers such as pH-responsive cholesteryl-bearing poly(amino acids),[10] photoresponsive spiropyrane-modified pullulan,[32] or thermoresponsive alkyl group modified poly(*N*-isopropylacrylamide)/CHP mixture.[33] The present study offers a new option in the design of functional nanogels by demonstrating that a change in the polysaccharide framework from linear to branched triggers subtle changes in the size and hydration level of the nanogels as well as in the microviscosity of their hydrophobic nanodomains. The exploitation of this new tool is under current investigation in our laboratory.

Acknowledgment. This work was supported by a Grant in Aid for Scientific Research from the Japanese government (No. 17300147) and CREST JST. The authors are grateful to Dr. S. Deguchi, Japan agency for Marine-Earth Science and Technology, for DLS measurements.

References and Notes

(1) *Biopolymers;* Vandamme, E. J., Bates, S. D., Steinbüchel, A., Eds.; Wiley-VCH Verlag GmbH: Weinheim, Germany, 2002.
(2) Rinaudo, M. *Macromol. Biosci.* **2006**, *6*, 590−610.
(3) Yashima, E. *J. Chromatogr., A* **2001**, *906*, 105−125.
(4) Finkenstadt, V. L. *Appl. Microbiol. Biotechnol.* **2005**, *67*, 735−745.
(5) *Polysaccharides for Drug Delivery and Pharmaceutical Applications*; Marchessault, R. H., Ravenelle F., Zhu, X. X., Eds.; American Chemical Society: Washington, DC, 2006.
(6) Akiyoshi, K.; Deguchi, S.; Moriguchi, N.; Yamaguchi, S.; Sunamoto, J. *Macromolecules* **1993**, *26*, 3062−3068.
(7) Akiyoshi, K.; Deguchi, S.; Tajima, H.; Nishikawa, T.; Sunamoto, J. *Macromolecules* **1997**, *30*, 857−861.
(8) Akiyoshi, K.; Sunamoto, J. *Supramol. Sci.* **1996**, *3*, 157−163.
(9) Kuroda, K.; Fujimoto, K.; Sunamoto, J.; Akiyoshi, K. *Langmuir* **2002**, *18*, 3780−3786.
(10) Akiyoshi, K.; Ueminami, A.; Kurumada, S.; Nomura, Y. *Macromolecules* **2000**, *33*, 6752−6756.
(11) Ringsdorf, H.; Venzmer, J.; Winnik, F. M. *Macromolecules* **1991**, *24*, 1678−1689.
(12) Kim, K.; Kwon, S.; Park, J. H.; Chung, H.; Jeong, Y.; Kwon, I. C. *Biomacromolecules* **2005**, *6*, 1154−1158.
(13) Park, K.; Kim, K.; Kwon, I. C.; Kim, S. K.; Lee, S.; Lee, D. Y.; Byun, Y. *Langmuir* **2004**, *20*, 11726−11731.
(14) Nichifor, M.; Lopes, A.; Carpov, A.; Melo, E. *Macromolecules* **1999**, *32*, 7078−7085.
(15) Nishikawa, T.; Akiyoshi, K.; Sunamoto, J. *J. Am. Chem. Soc.* **1996**, *118*, 6110−6115.
(16) Akiyoshi, K.; Sasaki, Y.; Sunamoto, J. *Bioconjugate Chem.* **1999**, *10*, 321−324.
(17) Nomura, Y.; Ikeda, M.; Yamaguchi, N.; Aoyama, Y.; Akiyoshi, K. *FEBS Lett.* **2003**, *553*, 271−276.
(18) Akihoshi, K.; Kobayashi, S.; Shichibe, S.; Mix, D.; Baudys, M.; Kim, S.W.; Sunamoto, J. *J. Controlled Release* **1998**, *54*, 313−320.
(19) Ikuta, Y.; Katayama, N.; Wang, L.; Okugawa, T.; Takahashi, Y.; Schmitt, M.; Gu, X.; Watanabe, M.; Akiyoshi, K.; Nakamura, H.; Kuribayashi, K.; Sunamoto, J.; Shiku, H. *Blood* **2002**, *99*, 3717−3724.
(20) Nakajima, T.; Ballou, C. E. *J. Biol. Chem.* **1974**, *249*, 7679−7684.
(21) Lehle, L.; Cohen, R. E.; Ballou, C. E. *J. Biol. Chem.* **1979**, *254*, 12209−12218.
(22) Vinogradov, E.; Petersen, B.; Bock, K. *Carbohydr. Res.* **1998**, *307*, 177−183.
(23) *Surfactant Solutions: New Methods of Investigation*; Zana, R., Ed.; Marcel Dekker: New York, 1987.
(24) Kalyanasundaram, K.; Thomas, J. K. *J. Am. Chem. Soc.* **1977**, *99*, 2039−2044.
(25) Lakowivz, J. R. *Principles of Fluorescence Spectroscopy*, 2nd ed.; Kluwer Academic/Plenum Publishers: New York, 1999.

(26) Turro, N. J.; Yekta, A. *J. Am. Chem. Soc.* **1978**, *100*, 5951−5952.
(27) Cehelnik, E. D.; Cundall, R. B.; Lockwood J. R.; Palmer. T. F. *J. Phys. Chem.* **1975**, *79*, 1369−1376.
(28) Lentz, B. R. *Chem. Phys. Lipids* **1989**, *50*, 171−179.
(29) Lentz, B. R. *Chem. Phys. Lipids* **1993**, *64*, 99−116.
(30) Kim, C.; Lee, S. C.; Kang, S. W.; Kwon, I. C.; Kim, Y. H.; Jeong, S. Y. *Langmuir* **2000**, *16*, 4792−4797.
(31) Lee, S. C.; Chang, Y. K.; Yoon, J. S.; Kim, C. H.; Kwon, I. C.; Kim, Y. H.; Jeong, S. Y. *Macromolecules* **1999**, *32*, 1847−1852.
(32) Hirakura, T.; Nomura, Y.; Aoyama, Y.; Akiyoshi, K. *Biomacromolecules* **2004**, *5*, 1804−1809.
(33) Akiyoshi, K.; Kang, E.-C.; Kurumada, S.; Sunamoto, J.; Principi, T.; Winnik, F. M. *Macromolecules* **2000**, *33*, 3244−3249.

BM070136Q